Intraplaque angiogenesis and therapeutic targeting of angiogenesis

Parma, L.

Chapter 4

Blockade of VEGF receptor 2 inhibits intraplaque hemorrhage by normalization of plaque neovessels

J Internal Medicine. 2018; 285(1):59-74.

MR de Vries[1,2]
L Parma[1,2]
EAB Peters [1,2]
A Schepers[1]
JF Hamming[1]
J Jukema[3]
MJ Goumans[4]
L Guo[5]
AV Finn[5]
R Virmani[5]
CK Ozaki[6]
PHA Quax[1,2]

[1]Department of Surgery, [2]Einthoven Laboratory for Experimental Vascular Medicine, [3]Department of Cardiology, [4]Department of Cell and Chemical Biology, Leiden University Medical Center, Leiden, The Netherlands. [5]CVPath Institute Inc. Gaithersburg, Maryland, USA. [6]Department of Surgery, Division of Vascular and Endovascular Surgery, Brigham and Women's Hospital, Harvard Medical School, Boston, Massachusetts, USA

Abstract

Background: Plaque angiogenesis is associated with atherosclerotic lesion growth, plaque instability and negative clinical outcome. Plaque angiogenesis is a natural occurring process to fulfill the increasing demand of oxygen and nourishment of the vessel wall. However, inadequate formed, immature plaque neovessels are leaky and cause intraplaque hemorrhage.

Objective: Blockade of VEGFR2 normalizes the unbridled process of plaque neovessel formation and induces maturation of nascent vessels resulting in prevention of intraplaque hemorrhage and influx of inflammatory cells into the plaque and subsequently increases plaque stability.

Methods and Results: In human carotid and vein graft atherosclerotic lesions, leaky plaque neovessels and intraplaque hemorrhage co-localize with VEGF/VEGFR2 and angiopoietins. Using hypercholesterolemic ApoE3*Leiden mice that received a donor caval vein interposition in the carotid artery we demonstrate that atherosclerotic vein graft lesions at t28 are associated with hypoxia, Hif1α and Sdf1 up-regulation. Local VEGF administration results in increased plaque angiogenesis. VEGFR2 blockade in this model results in a significant 44% decrease in intraplaque hemorrhage and 80% less extravasated erythrocytes compared to controls. VEGFR2 blockade *in vivo* results in a 32% reduction of vein graft size and more stable lesions with significantly reduced macrophage content (30%), and increased collagen (54%) and smooth muscle cell content (123%). Significant decreased VEGF, Angiopoietin-2 and increased Connexin 40 expression levels demonstrate increased plaque neovessel maturation in the vein grafts. VEGFR2 blockade in an aortic ring assay showed increased pericyte coverage of the capillary sprouts.

Conclusion: Inhibition of intraplaque hemorrhage by controlling neovessels maturation holds promise to improve plaque stability.

Graphical abstract

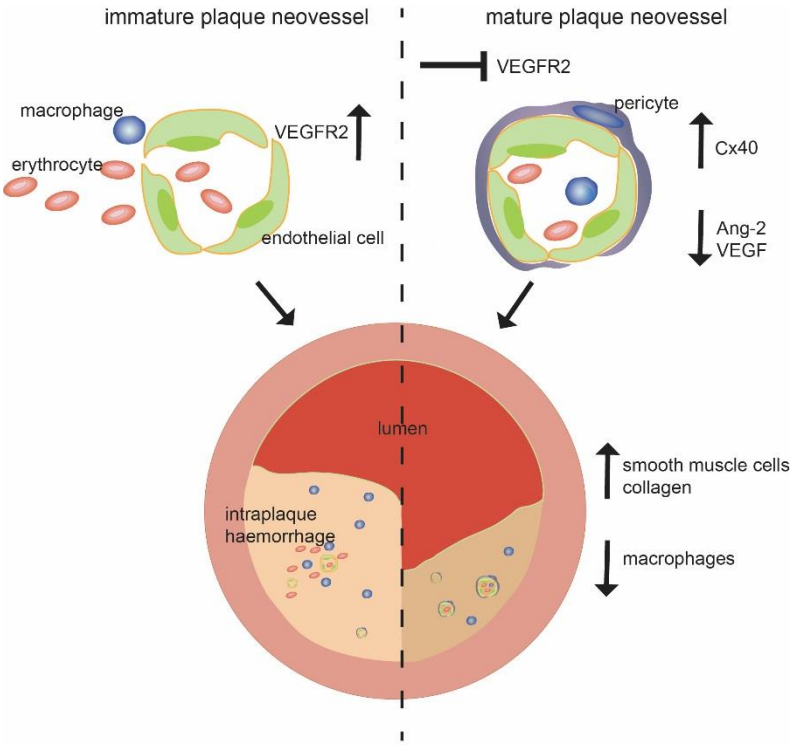

VEGFR2 blockade results in improved plaque neovessel maturation leading to reduced intraplaque haemorrhage and attenuated lesions with a more stable phenotype.

Introduction

Plaque angiogenesis and intraplaque hemorrhage are critical determinants of plaque instability [1]. Plaque angiogenesis or neovessel formation correlates with lesion progression, plaque inflammation and negative clinical outcome after cardiovascular events [2, 3]. Fragile atherosclerotic plaques do not only cause plaque instability in native atherosclerosis but also in post-interventional lesions such as in vein grafts and in in-stent neoatherosclerosis [4, 5].

Hypoxia in atherosclerotic lesions is a driver of plaque instability[6]. Furthermore, it can induce lesion growth and affect vascular remodeling[7, 8]. Angiogenesis a natural occurring process induced by hypoxia, fulfills the increasing demand of oxygen and nourishment of the vessel wall. Neovessel formation is stimulated by hypoxia-induced up-regulation of vascular endothelial growth factor (VEGF) [9, 10]. VEGF binds to and mediates its activity primarily through VEGF receptor 2 (VEGFR2). Plaque neovessels are frequently found dysfunctional especially, immature plaque neovessels. These neovessels are characterized by increased permeability caused by underdeveloped inter-endothelial junctions, incomplete basement membranes and partial pericyte coverage [11]. As a result, neovessels leak blood components into the lesions i.e. intraplaque hemorrhage. Erythrocytes in the plaque become phagocytosed and their cholesterol-rich membranes contribute to the free cholesterol content of the plaque [12-14]. Leaky neovessels are clearly associated with inflammatory cells[1]. Recently, it was shown by some of the coauthors that especially hemoglobin-haptoglobin receptor CD163+ macrophages interact with plaque neovessels and induce vascular permeability resulting in propagation of the instable character of lesions[15].

Anti-angiogenic therapies are used in cancer and eye diseases. However, these therapies are not always found beneficial [16]. Normalization of the neovasculature i.e. creating healthy mature neovessels is a relatively new strategy to target neovascularization [17]. Generation of a basement membrane and recruitment of pericytes are crucial steps in vessel maturation. These processes are regulated by VEGF-VEGFR2 and the tightly balanced angiopoietin-Tie2 system [18]. High levels of VEGF increase vessel permeability whereas low levels of VEGF are necessary for a stable vessel [19]. Angiopoietin (Ang)-1 mediates pericyte-endothelial cell adhesion and Ang-2 induces vessel permeability and acts as an antagonist to Ang-1, resulting in pericyte loss [19].

In preclinical models, it has been demonstrated that pro-angiogenic strategies augment atherosclerotic plaque growth and vascular inflammation whereas, anti-angiogenic strategies inhibit atherosclerosis [20-22]. Previously, we have shown that lesions induced by vein grafting in atherosclerosis-prone mice display profound plaque neovessels and intraplaque hemorrhage [23]. These plaque neovessels frequently lack pericyte coverage classifying them as immature [23].

We hypothesized that improving the maturation state of plaque neovessels reduces the extent of vascular “leakiness”, which results in reduced intraplaque hemorrhage and lesion progression. Since low levels of VEGF are necessary for vessel homeostasis, we investigated the impact of the VEGFR2 blocking antibody (DC101) on plaque angiogenesis, maturation status, and atherosclerotic lesion size and composition in murine vein grafts.

Materials and Methods

Human tissue specimens

Human coronary artery vein graft specimens (n=12) were available from the CVPath Institute. A detailed patient description can be found in table 1 of the on line supplement. The severity of the vein graft lesions were scored as early, intermediate or late as described previously[4]. Anonymous carotid endarterectomy (n=12) specimens obtained at the LUMC in accordance with guidelines set out by the 'Code for Proper Secondary Use of Human Tissue' of the Dutch Federation of Biomedical Scientific Societies (Federa) and conform with the principles outlined in the Declaration of Helsinki. The carotid endarterectomy specimens phenotype was scored based on the Athero Express Biobank classification[2]. Unstable plaques were selected based on relative necrotic core size, foam cell and inflammatory cell infiltration score, and the presence of neovascularization. Specimens were formalin fixed, embedded in paraffin, sectioned and stained as described below.

Animals

All animal experiments were performed in compliance with Dutch government guidelines and the Directive 2010/63/EU of the European Parliament. Male ApoE3*Leiden mice, crossbred in our own colony on a C57BL/6 background for at least 18 generations, 10-16 weeks old, were fed a diet (AB diets) containing 1% cholesterol and 0.05% cholate (VEGF experiment) or 0.5% cholate (time courses and DC101 experiment) from 3 weeks prior to surgery until sacrifice. The mice were housed on regular bedding and nesting material, water and diet were provided at libitum Mice were randomized based on their plasma cholesterol levels (inclusion criteria of cholesterol level >8 mM) (Roche Diagnostics, kit 1489437) and body weight. Mice were anesthetized with midazolam (5 mg/kg, Roche Diagnostics), medetomidine (0.5 mg/kg, Orion,) and fentanyl (0.05 mg/kg, Janssen Pharmaceutical). After the surgery, the anesthesia of the mice was antagonized with atipamezol (2.5 mg/kg, Orion) and fluminasenil (0.5 mg/kg, Fresenius Kabi). Buprenorphine (0.1 mg/kg, MSD Animal Health) was given after surgery to relieve pain.

Vein grafts

Vein graft surgery was performed by a donor caval vein interposition in the carotid artery of recipient mice as described before[23, 24]. At sacrifice, patency of the vein grafts was visually checked for pulsations and blood flow, occluded vein grafts were excluded from the study. animals underwent 3 minutes of *in vivo* perfusion-fixation with PBS and formalin under anesthesia. Vein grafts were harvested, formalin fixed, dehydrated and paraffin-embedded for histology.

Treatment

VEGF experiment: Immediately after vein graft surgery the vein graft was immersed *in vivo* in 100 µl of 40% pluronic gel (F127, Sigma Aldrich) containing 250 ng VEGF (n=7, Sigma Aldrich) or pluronic gel alone (n=6).

DC101 experiment: Mice were treated with IP injections of rat anti-mouse VEGF-R2 IgG monoclonal blocking antibodies (10 mg/kg DC101, Bio X cell)[25] (n=14) or control rat anti-mouse IgG antibodies (10 mg/kg, Bio X cell) (n=14) at day 14, 17, 21 and 25. 2 mice in this group were excluded from analysis due to thrombosis in the vein graft.

In vivo *detection of hypoxia*

One hour prior to sacrifice mice (n=6) received an intraperitoneal injection with the hypoxia marker pimonidazole hydrochloride (100 mg/kg, hypoxyprobe Omni kit, Hypoxyprobe Inc.). Pimonidazole was detected with the in the kit included rabbit polyclonal antibody (clone 2627).

Histological and immunohistochemical assessment of vein grafts

Cross sections were routinely stained with hematoxylin-phloxine-saffron (HPS) or Movat's pentachrome staining. Picrosirius red was used to detect collagen. The following antibodies were used for immunohistochemistry: endothelial cell CD31 (sc-1506-r, Santa Cruz), Glycophorin A (YTH89.1 Thermofisher), VEGF (sc-7269, Santa Cruz), VEGFR2 (55B11, Cell Signalling), Ang-1 (human; A78648, Atlas antibodies; murine LS-B62, LS Bio), Ang-2 (PAB19784, Abnova), intercellular adhesion molecule 1 (ICAM1 sc-1511-r, Santa Cruz), vascular cell adhesion protein 1 (VCAM1, ab27560, Abcam), stromal cell-derived factor 1 (SDF-1, ab9797, Abcam), Hypoxia-

inducible factor 1-alpha (HIF-1α, NB100-473, Novus Biologicals), CD163 (orb13303 Biorbyt), CD3 (ab16669, Abcam), macrophage MAC3 (550292, BD-Pharmingen), smooth muscle cell actin (SMCA, 1A4, Dako) and erythrocyte Ly76 (TER119, 116202, Biolegend). For each antibody isotype-matched antibodies were used as negative controls.

Images of the human lesions were obtained with the Ultrafast Digital Pathology Slide Scanner and associated software (Phillips). Bright field photographs were obtained with a Zeiss microscope and associated software. Fluorescent double and triple staining were acquired with the fluorescent slide scanner (3DHistech) and panoramic viewer software (3DHistech).

Morphometric analysis of vein grafts

Image analysis software (Qwin, Leica) was used for morphometric analysis. For each mouse eight (150 μm spaced) cross-sections were used to determine lesion size and occurrence of intraplaque hemorrhage over a total vein graft length of 1050 μm. Since elastic laminas are non-existent in these venous grafts, we analyzed the putative vessel wall area (or lesion area) by measuring total vessel area (area within the adventitia) and the lumen area. The lesion area was calculated as total vessel area minus lumen area. Immuno-positive areas in vein grafts are expressed as total area or percentage of the lesion area.

Morphologic analyses of intraplaque hemorrhage

Intraplaque hemorrhage was analyzed using CD31/Ly76 double-stained sections. Lesions where erythrocytes were found extravascular, adjacent to neovessels, were regarded as lesions with intraplaque hemorrhage. Using image analysis software (Qwin, Leica) the extravasated erythrocyte content was evaluate by measuring the total erythrocyte area in the lesion, followed by subtraction of the area of erythrocytes within the CD31 stained neovessels.

RNA isolation, cDNA synthesis and RT-PCR

Time course: total RNA was isolated from murine vein grafts harvested at several time points (vein grafts/time point; t0 (caval vein); 24h; 3d; 7d; (n=3 each), 14d (n=4) and 28d (n=5)). RNA was isolated and cDNA was synthesized as described previously[26].

VEGFR2 experiment: total RNA was isolated from 10 (20µm thick) paraffin sections of vein grafts (n=6/group). RNA was isolated according manufacturers protocol (FFPE RNA isolation kit, Qiagen). RNA for Q-PCR was reverse transcribed using a High Capacity RNA-to-cDNA kit (Applied Biosystems). Commercially available TaqMan gene expression assays for the housekeeping gene hypoxanthine phosphoribosyl transferase (HPRT1), and selected genes were used (Applied Biosystems); *Vegfa* (Mm 00437306_m1), *Hif1-α* (Mm 0468869_m1), *Sdf-1 (Mm 00445553_m1), Vegfr2* (Mm01222421_m1), *Vegfr1* (Mm00438980_m1), *Tie2* (Mm00443243_m1), *Icam1* (Mm00516023_m1), *Ang-1* (Mm00456503_m1), *Ang-2* (Mm00545822_m1), *Connexin37* (Mm01179783_m1), *Connexin40* (Mm01265686_m1), *Connexin43* (Mm00439105_m1), *Ccl2* (Mm00441242_m1) and *Il6* (Mm00441242_m1)). Q-PCRs were performed on the ABI 7500 Fast system (Applied Biosystems). The 2-ΔΔCt method was used to analyze the relative changes in gene expression.

Aortic ring assay

3 separate experiments were conducted using 3 mice per experiment. C57BL/6 mice, age between 8- 12 weeks, were anesthetized (as described above) and the aorta was dissected and stored in medium. Each aorta was cut in 1 mm rings, and serum-starved in Opti-MEM + Glutamax (Gibco) overnight at 37 °C and 5% CO2. The next day, each ring was mounted in a well of a 96-well plate in 70 µl of 1.0 mg/ml acid-solubilized rat tail collagen I (Millipore) in DMEM. After collagen polymerization (60 min at 37 °C and 5% CO2), Opti-MEM supplemented with 2.5% FCS and 30 ng/ml VEGF (R&D systems) was added with or without DC101 or control antibodies (30 µg/ml). The rings were cultured for 7 days and pictures were taken (Zeiss). The number of sprouts were counted manually.

For immunohistochemistry rings were formalin fixed and permeabilized with 0.2% Triton X-100. Rings were stained with SMCA, CD31 (BD Pharmingen) and MAC3. Z stack images were captured with a LSM700 confocal laser-scanning microscope (Zeiss) and quantified with image J.

Statistical analysis

Results are expressed as mean ± SEM. A 2-tailed Student's t-test was used to compare individual groups. Non-Gaussian distributed data were analyzed using a Mann-Whitney U test using

GraphPad Prism version 6.00 for Windows (GraphPad Software). Probability-values <0.05 were regarded significant.

Results

Leaky neovessels in human vein graft and carotid lesions

Both vein graft specimens (Fig 1 panel 1) and carotid atherosclerotic lesions (Fig 1 panel 2) show features of classical atherosclerotic lesions with, foam cells, calcification and necrotic cores. Neovessels were found throughout the lesions in both vein grafts and carotid specimen, with preference for the media and at inflammatory regions around necrotic cores, Fig 1B panel 1&2. Frequently, these neovessels were leaky as demonstrated by the presence of erythrocytes (Glycophorin A expressing cells) outside the neovessels, Fig 1C panel 1&2. Both Ang-1 (Fig 1D panel 1&2) and Ang-2 (Fig 1E panel 1&2) were localized around the neovessels, although not all neovessels were found positive. Most neovessels, also in regions of intraplaque hemorrhage, did express VEGF, Fig 1F panel 1&2. VEGFR2 staining was present around the neovessels but not as strong as VEGF expression, Fig 1G panel 1&2.

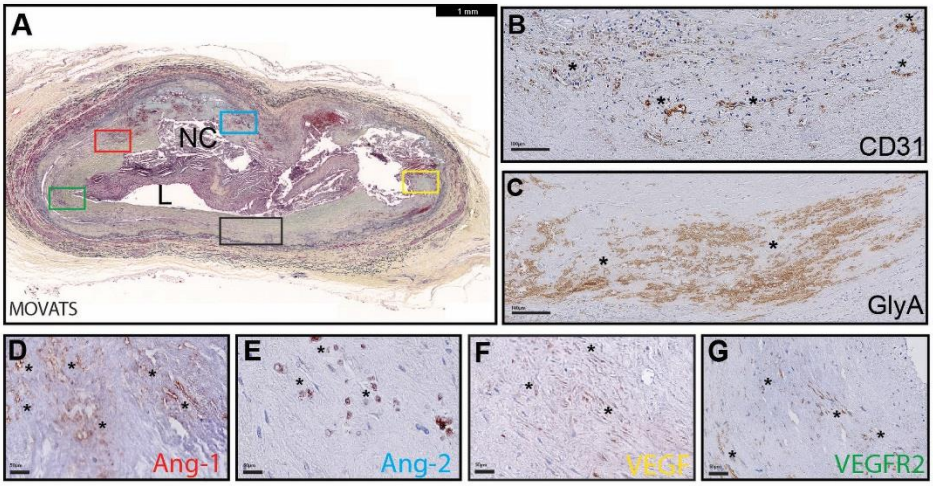

Panel 2 Carotid lesion

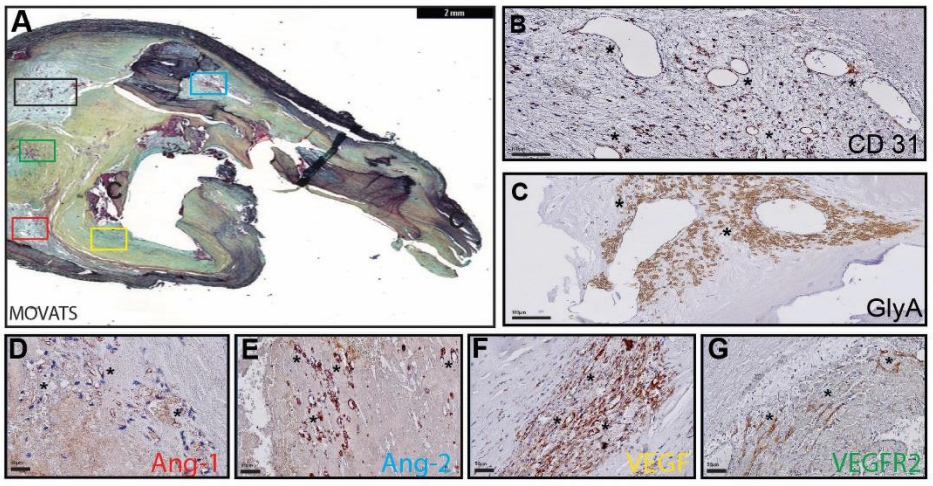

Figure 1. Leaky neovessels in human vein graft and carotid lesions. (A) Human vein grafts (n=12) and (B) carotid plaques (n=12) were stained with Movat's pentachrome for general morphology. (A/B.1) CD31 positive leaky neovessels as revealed by the presence of (A.2/ B.2) glycophorin A (GLyA) positive erythrocytes outside neovessels. (A.3-4, B.3-4) Angiopoietins, Ang-1 and Ang-2, localized around the neovessels as well as VEGF and VEGFR2 (A.5-6, B.5-6). NC, necrotic core. L, Lumen C, Calcification. *neovessels.

Hypoxia drives plaque angiogenesis in vein grafts

In a time-course experiment of murine vein grafts the expression of *Hif1-α* mRNA rapidly and significantly increased in vein grafts at all time points until day 28 (t28), when compared to native caval veins, with the highest level at t7, Fig 2A. *Hif1-α* protein expression was clearly visible at t28, Fig 2B. *Sdf-1* mRNA was significantly up regulated from t7 to t28 when compared to caval veins, Fig 2C. At the latter time point, *Sdf-1* protein expression could be detected especially in SMCs, Fig 2D. Interestingly, while we could not detect an increase of *Vegf-a* mRNA during the time-course, Fig 2E, positive VEGF staining could be seen at t28, especially in plaque neovessels, Fig 2F. *In vivo* we determined hypoxia by injecting the hypoxia probe pimonidazole (n=6). Hypoxia was evident in all layers of the vein graft (t28), especially in macrophages scattered throughout the vein graft, Fig 2G and H.

A histological time course of vein grafts was used to study the timeframe in which the first plaque neovessels appear. From t14 (n=4) the first plaque neovessels were detectable. These neovessels were primarily in the outer region of the vein grafts, suggesting sprouting from the vasa vasorum, Fig 2I. At t28 $CD31^{+}$ plaque neovessels could be detected throughout all layers of the vein graft (n=4), Fig 2J. The majority of these plaque neovessels have an activated endothelium, demonstrated by the expression of ICAM1 (Fig 2K) and VCAM1, Fig 2L. Up regulation of ICAM1 and VCAM1 can lead to increased interactions with inflammatory cells. Therefore, 28 days old vein grafts were stained with a combination of CD31 and CD163, an exclusive marker for neovessel associated macrophages[15] and CD31 and CD3+T cells. CD163+ macrophages can be abundantly found throughout the vein graft lesion (Fig 2M) but mostly in close proximity of neovessels (Fig 2N). CD3+ T cells are mainly located in the peri-adventitial region of the vein grafts which are highly vascularized (Fig 2O,P).However, CD3+ T cells are not specifically associated with neovessels in other areas within the vein graft lesion (white arrow, Fig 2O).

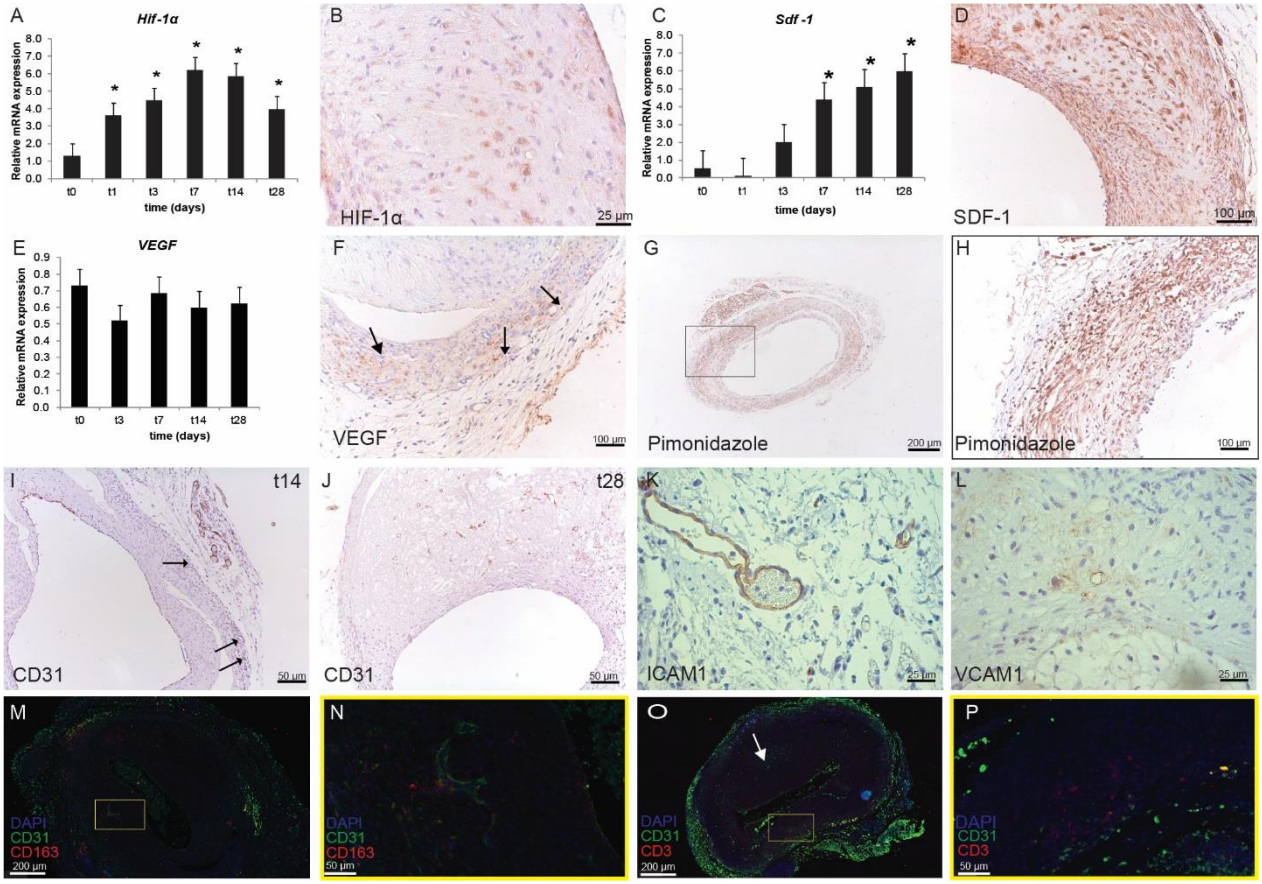

Figure 2. Hypoxia drives plaque angiogenesis. (A) Hypoxia inducible factor (Hif)-1α mRNA regulation over time in vein grafts (t0-t7 n=3, t14 n=4, t28 n=5) in hypercholesterolemic ApoE3*Leiden mice. **(B)** HIF-1α protein is expressed by various cell types in vein grafts (t28). **(C)** Stromal cell-derived factor 1 (Sdf-1) mRNA regulation over time. **(D)** At day 28 SDF-1 is expressed in all layers of the vein graft. **(E)** Vegf mRNA regulation over time. (**F**) VEGF could be seen in neovessels (arrows) in the vessel wall (t28). **(G,H)** Hypoxia (t28) could be detected with pimonidazole throughout the vein graft wall (n=6 mice). **(I)** In a histological time course (n=4 mice/time point) neovessels expressing CD31 could be detected from day 14 (t14) onwards. **(J)** At t28 neovessels could be detected throughout the entire vessel wall. Plaque neovessels show activation by expression of Intercellular Adhesion Molecule 1 (ICAM1) **(K)** and Vascular Cell Adhesion Molecule 1 (VCAM1) **(L)**. CD163+ macrophages are found throughout the t28 vein graft lesion **(M)** and are clearly associated with neovessels **(N)**. CD3+ T cells are found in the peri-adventitial region of the vein grafts but not so much in other regions (white arrow) associated with neovessels **(O,P)** * $p<0.05$

Perivascular VEGF increases plaque neovessel density

To examine whether in the vein graft model we could target plaque angiogenesis we applied, a pluronic gel containing 250 ng VEGF in the perivascular region of the vein grafts, directly after surgery. Local treatment with VEGF did not affect cholesterol levels or bodyweight, S1A and B. After 28 days, we observed an increase in the number of neovessels in the VEGF treated group compared to controls, Fig 3A. Quantification of the plaque neovessel density per section revealed a significant 60% increase in neovessels in the VEGF group ($p=0.014$), Fig 3B. However, local

application of VEGF did not result in a significant effect on the vessel wall area (p= 0.628), Fig 3C. Both in the control group as well as in the VEGF treated group 1 out of 6 mice intraplaque hemorrhage was observed.

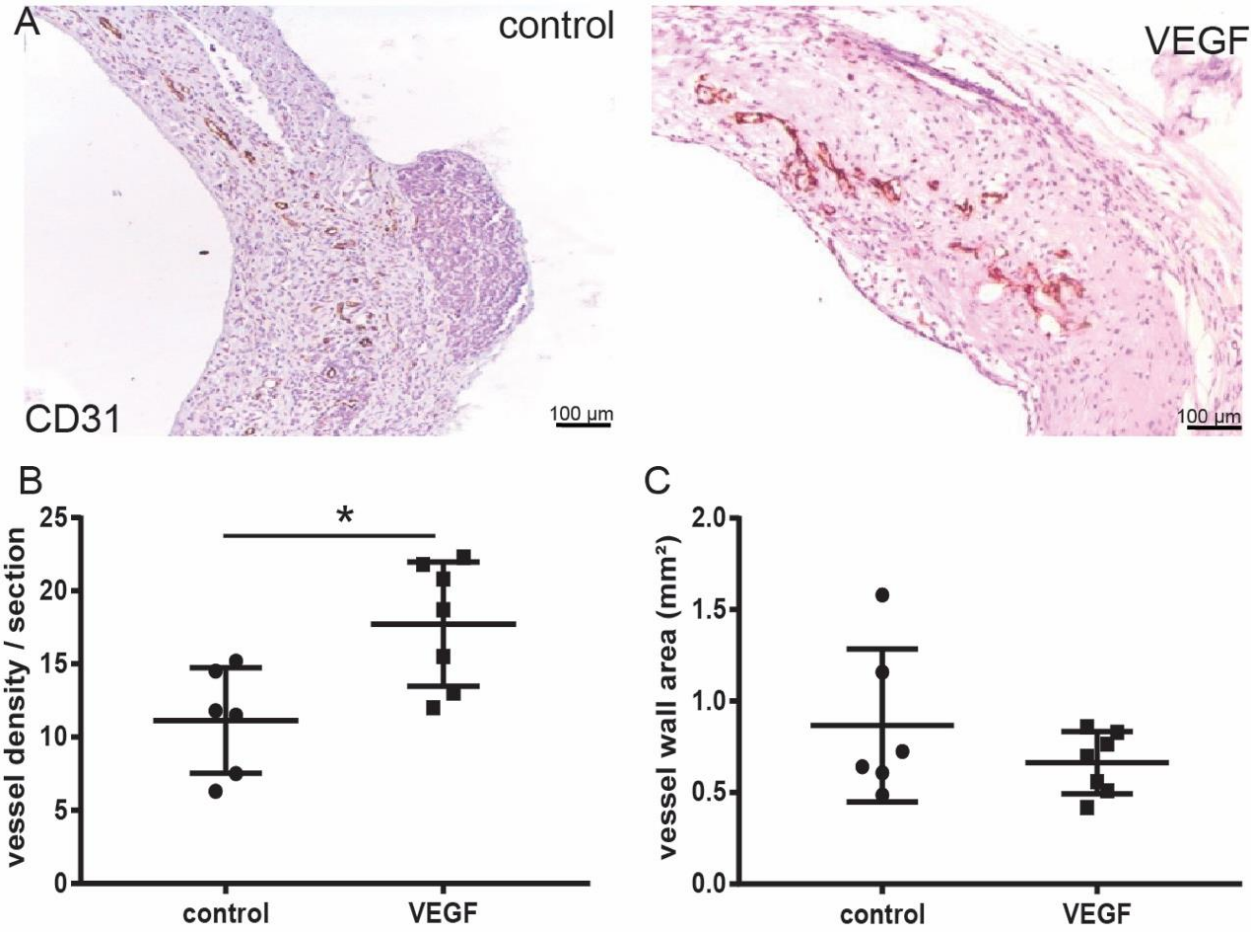

Figure 3. Perivascular VEGF increases plaque angiogenesis. VEGF was applied in pluronic gel (n=7) or pluronic gel alone (n=6) topically on the vein in ApoE3*Leiden mice. **(A)** CD31 staining of plaque neovessels in the control group (n=6) and VEGF group (n=7). **(B)** Quantification of the neovessel density at day 28 **(C)** Quantification of the vessel wall area. * p<0.05

Angiopoietin expression is augmented in intraplaque hemorrhage regions

Neovessels associated with intraplaque hemorrhage are characterized by reduced pericyte coverage. Mature neovessels are covered by SMC actin positive pericytes, Fig 4A. In regions of intraplaque hemorrhage (characterized by perivascular erythrocytes) neovessels were partly devoid of pericyte coverage, Fig 4B. Tie2, the main receptor of the angiopoietins was found to be specifically expressed by endothelial cells of plaque neovessels. The expression of Tie2 did not

differ between mature neovessels (Fig 4C) or neovessels associated with intraplaque hemorrhage, Fig 4D. Increased staining of both Ang-1 and Ang-2 could be observed in areas of intraplaque hemorrhage. Ang-1 was predominantly expressed in intraplaque hemorrhage regions whereas no staining around mature neovessels could be observed, Fig 4E. Ang-2 showed increased expression in lesions with intraplaque hemorrhage in contrast to regions of the lesions without intraplaque hemorrhage, Fig 4F.

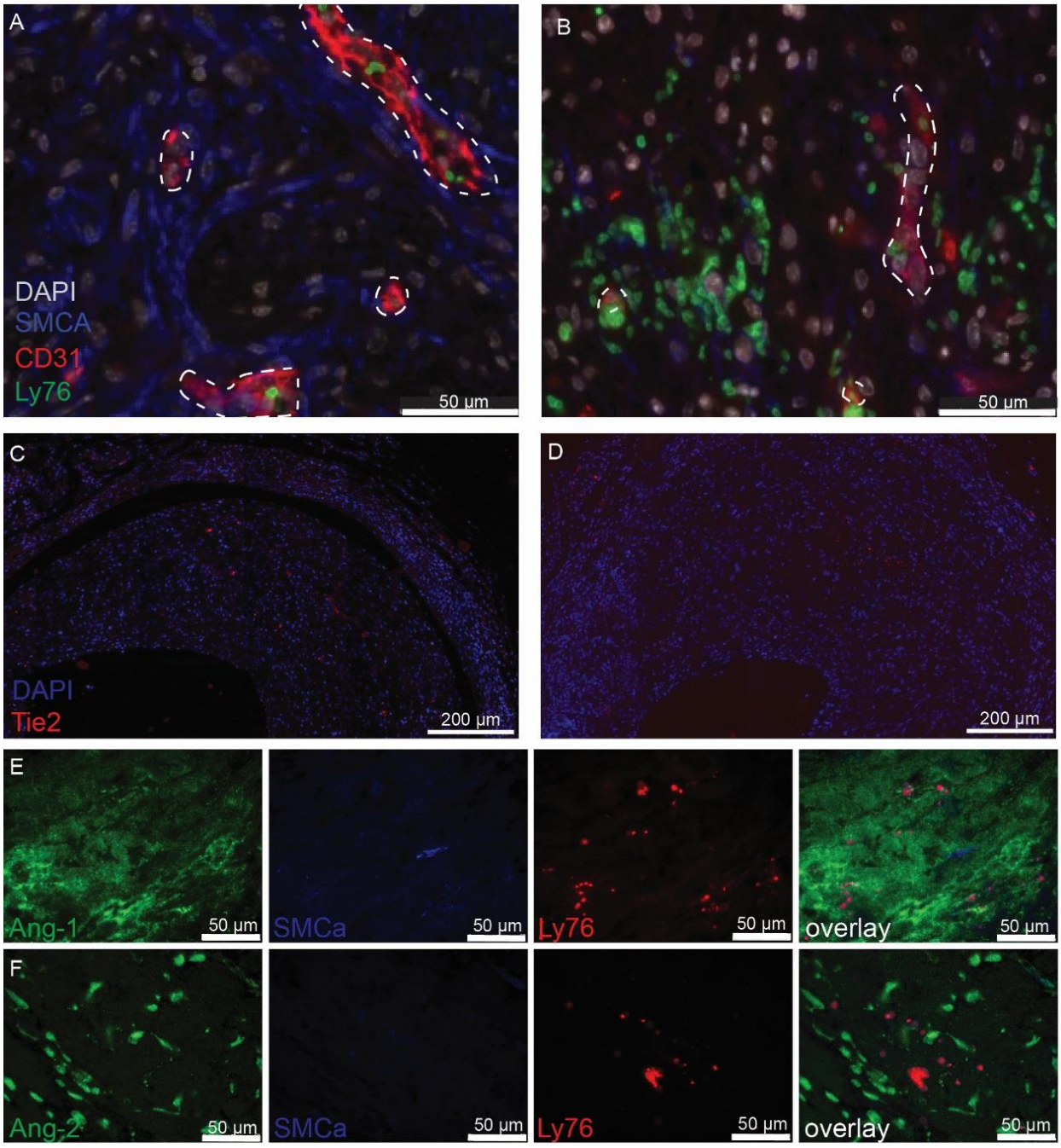

Figure 4. Angiopoietins-Tie2 expression in regions of intraplaque hemorrhage. (A) Staining of smooth muscle cell actin (SMCA), endothelial cells (CD31) and erythrocytes (Ly76) in plaque neovessels (dashed white lining) in lesion without (left panel) and with (right panel) intraplaque hemorrhage (IPH). **(B)** Staining of Tie2 in lesion without (left panel) and with (right panel) IPH. **(C)** Single staining's and overlay of Angiopoietin (Ang)-1 (Ang-1), SMCA and Ly76 in regions of IPH. **(D)** Single staining's and overlay of Ang-2, SMCA and Ly76 in regions of IPH.

VEGFR2 blocking antibodies inhibit intraplaque hemorrhage and erythrocyte extravasation

To interfere in the process of vessel integrity, we treated ApoE3*Leiden receiving a vein graft with the VEGFR2 blocking antibody (DC101). Treatment with DC101 did not change cholesterol levels or bodyweight in comparison to the control group, S1C and D. Intraplaque hemorrhage was less frequently observed in mice treated with DC101 (7 out of 14 mice, 50%) in comparison to control animals (10 out of 12 mice, 83%). In the DC101 group a smaller segment of the vein grafts (242 µm, 26% of the vein graft length) was affected by intraplaque hemorrhage in comparison to the control group (620 µm, 59% of the vein graft length, p=0.037), Fig 5A. In addition, 80% less extravasated erythrocytes were observed in the DC101 group than in the control group (p=0.049), Fig 5B. These extravasated erythrocytes were predominantly observed in the regions near the adventitia and in the mid-portion of the vein graft lesions, Fig 5B.

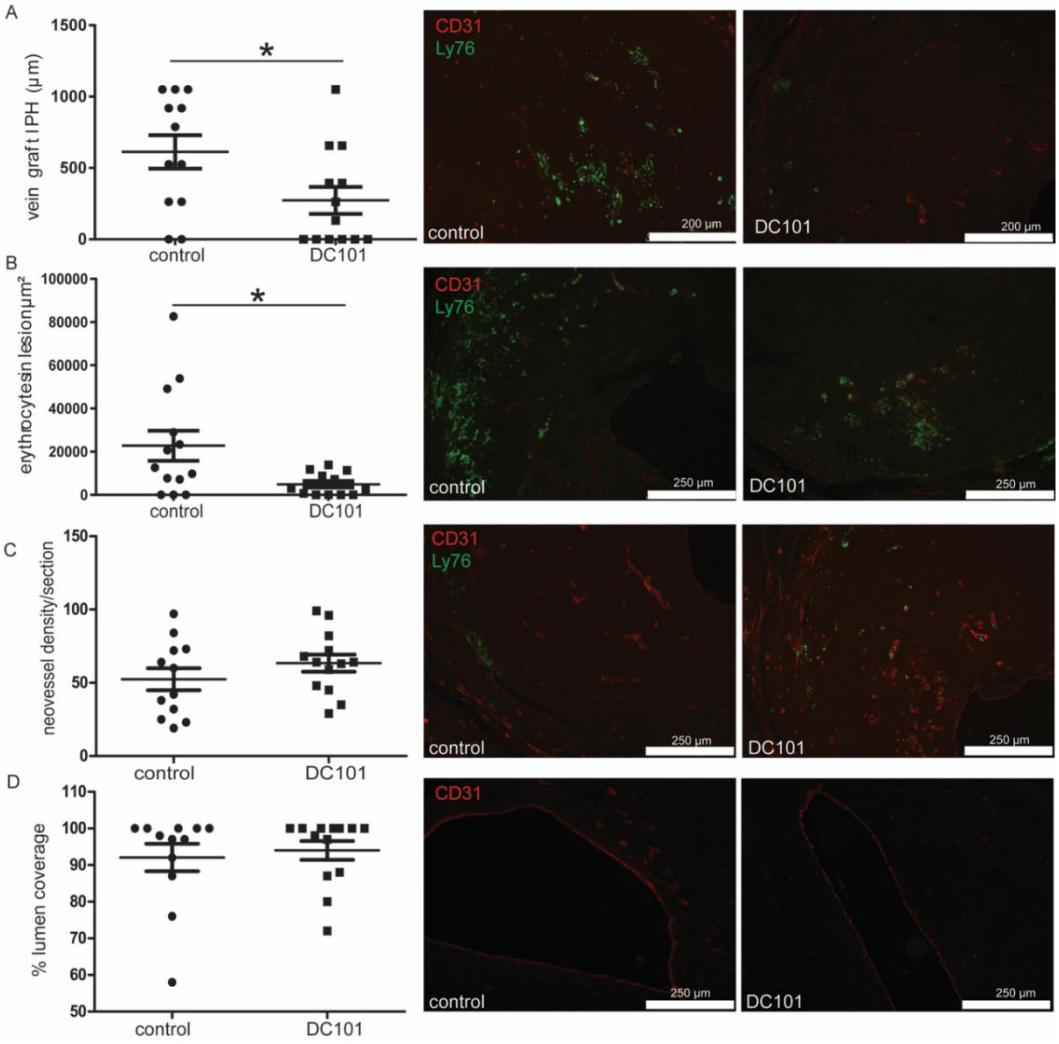

Figure 5. Intraplaque hemorrhage and erythrocyte extravasation after VEGFR2 blockade. Vein grafts in hypercholesterolemic ApoE3*L mice treated with control IgG antibodies (10 mg/kg) n=12 and VEGFR2 blocking antibodies (DC101, 10 mg/kg) n=14, 28 days after surgery **(A)** Quantification of the vein graft length that displayed intraplaque hemorrhage. Representative examples of lesions with intraplaque hemorrhage. **(B)** Quantification of the area of the extravasated erythrocytes and representative images of lesions with extravasated erythrocytes. **(C)** Quantification of the density of neovessels in vein grafts expressed as the number of neovessel per section (10-12 sections/mouse) **(D)**. Quantification of endothelial cell coverage of the lumen expressed as % coverage. * $p<0.05$, L = lumen.

Neovessel density is not reduced by VEGFR2 blocking antibodies in vivo

The anti-angiogenic effect of suppression of VEGF-signaling *in vivo* was analyzed by quantifying the neovessel density in the vein graft lesions. In the DC101 group an average of 63±25 neovessels per vein graft section was observed, whereas in the control IgG treated group 52±19 neovessels per vein graft section were found (p=0.327), Fig 5C. The vein graft model is characterized by denudation of the luminal endothelium in the early days after engraftment, which is restored later in time[5]. Both in the DC101 group and the control group the endothelium was completely restored at 28 days after surgery (p=0.639), Fig 5D.

DC101 prevents vein graft thickening and results in a more stable lesion composition

VEGFR2 blockade resulted in a reduction of the lesion size compared to the control group, Fig 6A. Quantification of these lesions showed that the DC101 treated group had a significant reduction of 32% in vein graft thickening compared to the control IgG treated group (p=0.044), Fig 6A. A decrease in outward remodeling as measured by the total vessel area, was detected in the DC101 treated group (33%, p=0.05), S2A. The luminal area however, was not significantly affected by DC101 treatment (p=0.369), S2B. Next, the effect of DC101 treatment on vein graft lesion composition was assessed. In the DC101 group an increased collagen content was observed in comparison to the control group (46%, p=0.066), S2C. When corrected for the differences in vein graft thickening, the relative percentage of collagen was significantly increased in the DC101 treated group (54% p=0.047), Fig 6B. In addition, a substantial increase in the SMCA area was observed (118% p=0.003) in the DC101 group as well as a significant increase in the percentage of SMCA (123% p=0.0005), Fig 6C and S2D. Plaque macrophages were significantly reduced after DC101 treatment with 30% (p=0.001), Fig 6D whereas, the total macrophage area was reduced by 42% (p=0.018), S2E.

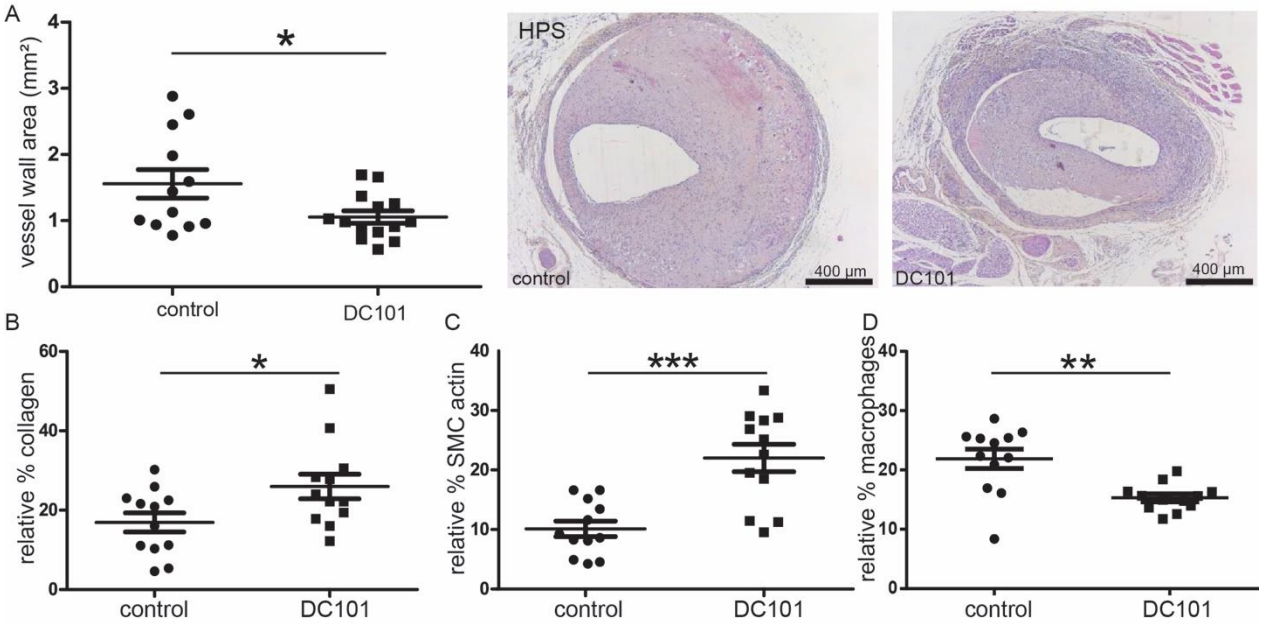

Figure 6. Quantitative measurements of vein graft area and lesion composition. (**A**) Quantitative measurements of vein graft thickening and representative cross-sections of vein
grafts in hypercholesterolemic ApoE3*L mice treated with control IgG antibodies (10 mg/kg) n=12 and VEGFR2 blocking antibodies (DC101, 10 mg/kg) n=14, 28 days after surgery (Hematoxilin-Phloxine-Saffron staining). **(B)** relative percentage collagen, **(C)** relative percentage smooth muscle cell actin, **(D)** relative percentage macrophages. * p<0.05, **p<0.01, ***p<0.005.

VEGFR2 blockade stimulates expression of genes associated with a more mature neovessel phenotype

To investigate the local inflammatory response, we measured the gene expression levels of pro-inflammatory genes *Ccl2, Il6* and *Icam1* in the vein grafts; No differences in expression levels could be detected between the groups, Fig 7A-C. Also, the expression of VEGF/VEGFR mRNA in the vein graft wall was analyzed. Interestingly, the expression of both *Vegfa* (Fig 7D) and *Vegfr1* (Fig 7E) was significantly reduced upon DC101 treatment (24% (p=0.014) and 32% (p=0.048) respectively) whereas, the expression of *Vegfr2* was not affected, Fig 7F. Furthermore, the angiopoietin receptor *Tie2* (Fig 7G) was not differently expressed between the groups, nor was the vessel stabilizing factor *Ang1*, Fig 7H. The vessel destabilizing factor *Ang2* was significantly decreased (p=0.039) after DC101 treatment, Fig 7I. As a measure for proper endothelial function, we measured Connexin (*Cx*43, *Cx37* and *Cx40*) expression. DC101 treatment showed no effect on *Cx43* (Fig 7J) and *Cx37* (Fig 7K) expression levels but remarkably, significantly increased (p=0.047) levels of *Cx40* were observed pointing towards increased inter-endothelial cell connections, Fig 7L.

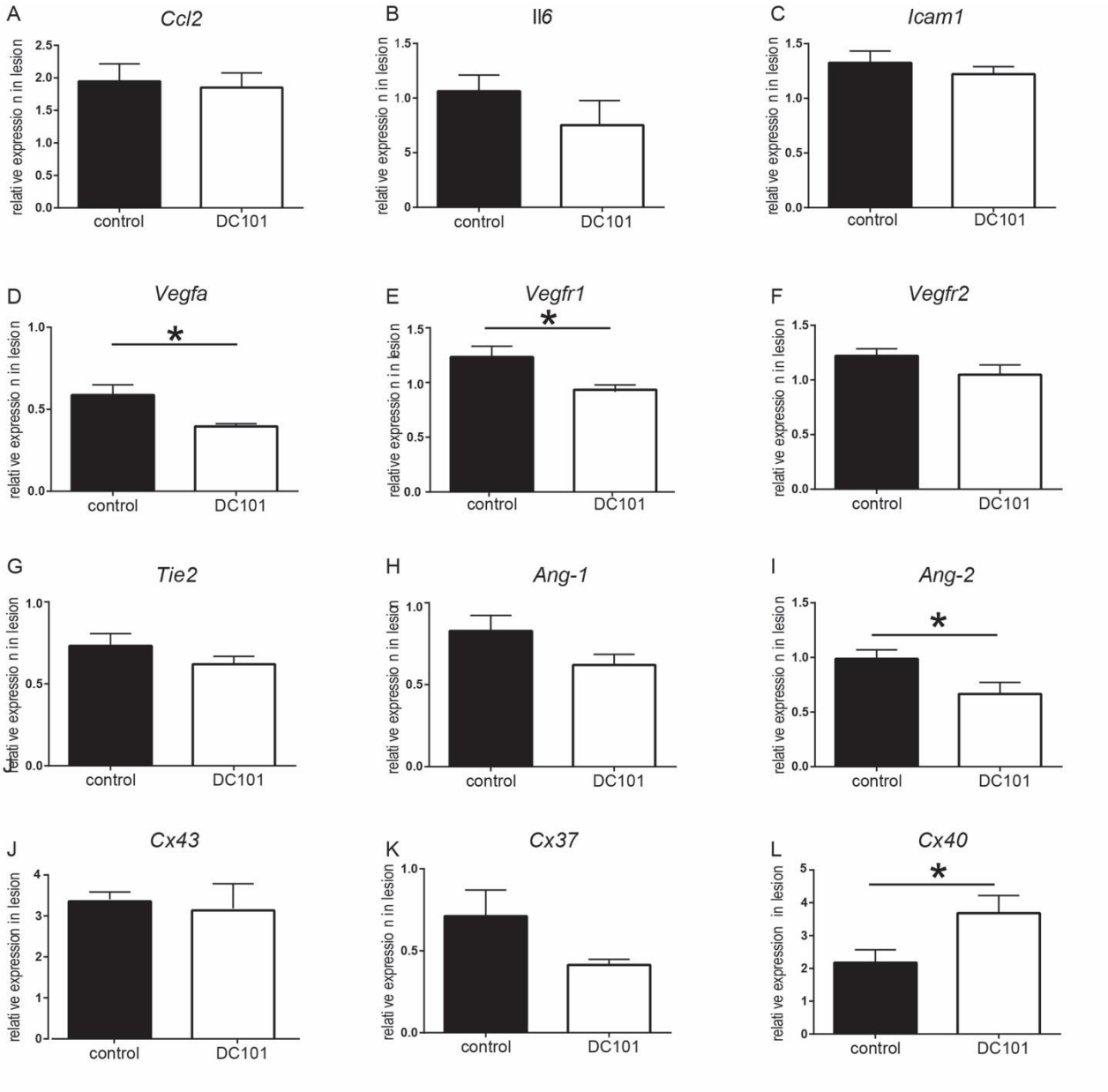

Figure 7. Gene expression in vein grafts. Total wall gene expression was measured in vein grafts of control and VEGFR2 blocking antibodies treated mice (n=6/group). **(A)** Inflammation associated genes. **((B)** VEGF and VEGF receptor genes. **(C)** Tie2 and angiopoietins. **(D)** Connexins. *p<0.05.

VEGFR2 blocking antibodies induce concentration dependent vessel maturation

The effects of VEGFR2 blockade on vessel maturation was further studied in an aortic ring assay. Of the 2 concentrations DC101(10 and 30 µg/ml) tested, only the highest concentration resulted

in a significant reduction (66% p=0.003) of sprout formation when compared to no treatment, Fig 8A. The pericyte coverage of the sprout in the 30 µg/ml DC101 group was not significantly different than the control. Interestingly, the 10 µg/ml DC101 concentration induced a significant increase in SMCA^{+} pericyte coverage of the CD31^{+} sprouts (20%, p=0.005), Fig 8B and C.

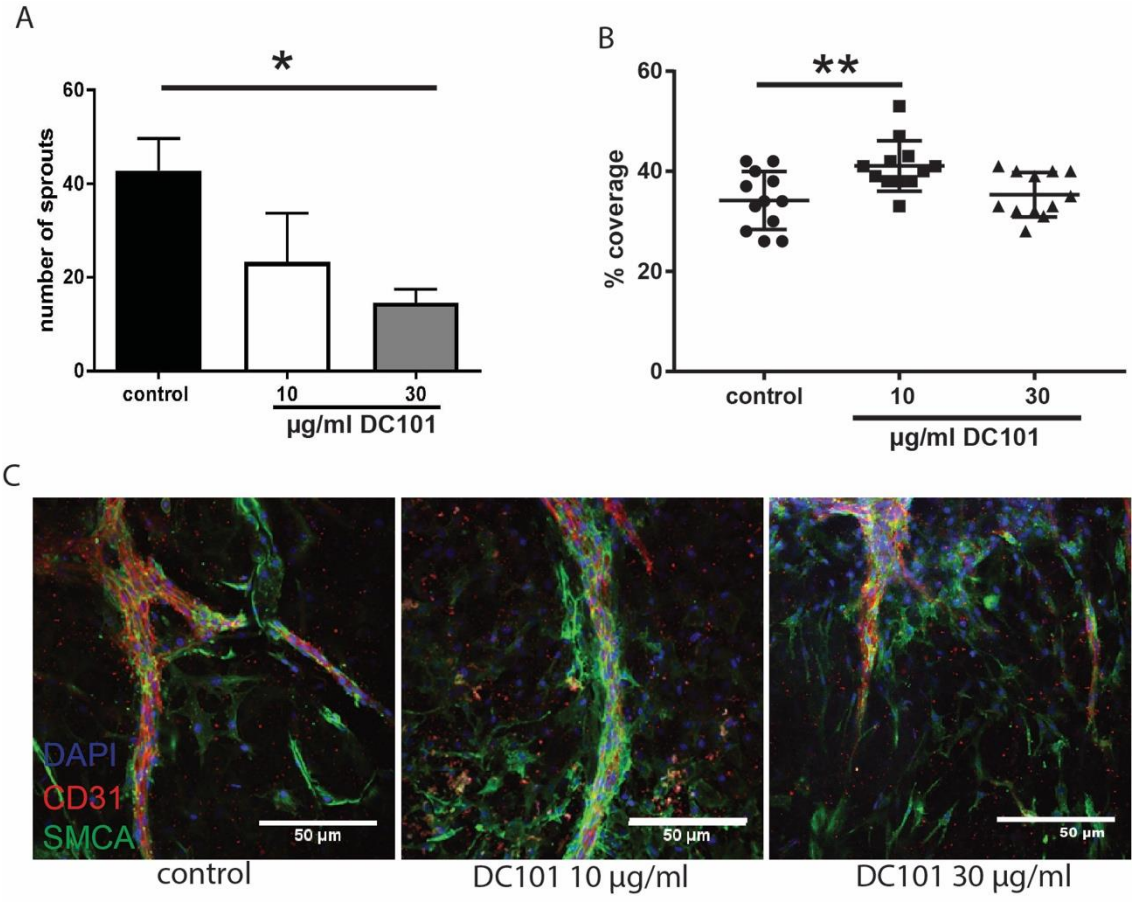

Figure 8. VEGFR2 blockade in aortic ring assay. Representative experiment of 3 separate experiments using 3 mice/condition and 4 rings per mouse. Quantification of the number of sprouts **(A)** and the % coverage of SMCs over the CD31^{+} sprouts **(B)**. **(C)** Typical examples of sprouts in the control and DC101 treated groups. * p<0.05, ** p<0.01.

Discussion

Immature intraplaque neovessels have been characterized as the main contributors to intraplaque hemorrhage. Intraplaque hemorrhage occurs in native atherosclerosis but also in accelerated atherosclerosis after vein grafting or stenting[4]. However, most of the evidence is descriptive in nature [9, 13]. In the present study, we used an intervention to show that VEGFR2 blockade reduces intraplaque hemorrhage and increases plaque stability by enhancing neovessels maturation in vein graft atherosclerosis.

We observed that neovessels in human carotid and vein graft specimen are associated with VEGF/VEGFR2 and angiopoietins. In both types of atherosclerotic lesions numerous regions with intraplaque hemorrhage and leaky vessels were observed. We demonstrated that plaque neovessels in the vein grafts originate primarily from the adventitia, This is also the general idea for native atherosclerotic lesion however, luminal angiogenesis cannot be excluded [1]. VEGFR2 is involved in this process as the main receptor. VEGFR2 is involved in tip-cell-stalk-cell differentiation in the early phase of angiogenesis and mediates the permeability enhancing effects of VEGF in adult endothelial cells as well as neovessel maturation [16]. We have previously shown that the majority of plaque neovessels in vein grafts express a basement membrane and that pericytes coverage is heterogeneous [23]. Here we demonstrate that incomplete pericyte coverage of murine plaque neovessels is angiopoietin related. Incomplete pericyte coverage in regions of intraplaque hemorrhage is also observed in human instable atherosclerotic plaques [11].

A modest induction in Vegf mRNA expression between 3 and 7 days but no further regulation between other time points was observed. Interestingly, Hamdan et al. showed comparable absent induction of Vegf mRNA in a canine vein graft model between native vein and 4 weeks after surgery, but did see a significant induction after 48 hours [27]. It seems that Vegf mRNA expression is only induced for a short period and is not the main driver of the remodeling response after vein graft surgery. This early induction of Vegf mRNA expression can be a result of the hypoxic period during surgery.

Atherosclerotic plaque angiogenesis can be manipulated as we show here by intervening in the VEGF pathway: locally applied VEGF enhanced neovessel density. We found that low

concentration of VEGFR2 blocking antibodies induced pericyte coverage in the aortic ring assay. This is comparable to the observation of increased pericyte coverage in murine and human tumors after VEGF signal blockade [28]. Blockade of VEGFR2 has been shown to facilitate the recruitment of pericytes to tumor vessels by enhancing Ang-1 expression and increasing perivascular matrix metalloproteases activity [29]. Ang-1 decreases endothelial cell permeability and increases vascular stabilization via enhancing endothelial cell interactions with the surrounding matrix and recruitment of pericytes to growing blood vessels. Ang-2 functions as a competitive Ang-1 antagonist in a VEGF-depend manner and mediates angiogenic sprouting and vascular regression [19]. This concurs with our finding that in regions of intraplaque hemorrhage the expression of both Ang-1 and Ang-2 is increased. VEGFR2 blockade by DC101 treatment reduced intraplaque hemorrhage, reduced *Ang-2* expression, and improving gap junctions as shown by the increased *Cx40* expression, pointing towards more mature neovessels. Post *et al*. showed that in plaques with high neovessel density, the local balance between Ang-1 and Ang-2 is in favor of Ang-2 [30]. Unfortunately, vascular maturation and intraplaque hemorrhage was not studied in this context.

Recently, it was shown that treatment with axitinib (inhibitor of VEGFR1,2, and 3) attenuated plaque angiogenesis [31]. Treating vein grafts with VEGFR2 blocking antibodies *in vivo* did not result in a reduction of neovessel density in comparison to control IgG treated animals. Interestingly in a model for breast cancer, tumor vascular density was also not affected with this dose (10 mg/kg DC101) but was significant decreased with a four times higher dose [32]. Furthermore, these authors observed that low dose but not high dose VEGFR2 blocking antibodies treatment resulted in improved vascular maturation. In the aortic ring assay, we observed that the high dose DC101 resulted in reduced sprouting whereas the low dose did not reduce sprouting but did increased pericyte coverage.

VEGF is known to induce re-endothelialization and has been shown to inhibit intimal hyperplasia after vascular injury [33]. Application of VEGF directly after surgery in a rabbit vein graft model showed attenuation of the vessel wall size [34]. We show that local delivery of VEGF directly after surgery results in a non-significant trend towards reduction of intimal hyperplasia. Whereas, blockade of VEGFR2 resulted in significant attenuation of lesion growth. In the VEGFR2 blockade

experiment, treatment with DC101 was started at day 14 after surgery to specifically study the effects on plaque neovessel formation which starts from this time point on as demonstrated in Fig 2I. An important mechanism of action of VEGF is enhancing the re-endothelialtization of the luminal endothelium which occurs primarily in the early period after surgery [35]. The late treatment with DC101 does not interfere with the re-endothelialization process. This was confirmed by the observation that at sacrifice (t=28 days) both the control and DC101 group showed full luminal endothelial coverage. Vein graft lesion formation is largely driven by inflammation [36]. The positive effect of VEGFR2 blockade on this process most likely overrules the VEGF induced attenuation of lesion growth.

It has been shown that VEGFR2 activation can activate and degrade VE-cadherin resulting in vascular permeability [37]. Guo et al showed that CD163+ macrophages promote endothelial permeability via VEGF/VEGFR2 interaction with VE-cadherin [15]. These CD163+ macrophages are clearly present, localized in areas of plaque neovascularization, in the murine vein grafts (Fig 2). Blockade of VEGFR2 could reverse the VE-cadherin induced vascular permeability and induce the observed plaque neovessel maturation and reduced intraplaque hemorrhage.

Phagocytosis of intraplaque erythrocytes and erythrocyte–derived cholesterol by macrophages results in lipid core and plaque expansion, and promotion of plaque instability [12, 38]. Systematic VEGFR2 blockade led to a reduction of intraplaque hemorrhage, lesion size and a reduction in lesion macrophages. Binding of VEGF to VEGFR2 can result in NF-κB induced activation of VCAM-1 and ICAM-1 leading to increased adherence of leukocytes [39]. In various experimental models, inhibition of vascular leakage and NF-κB dependent macrophage influx by DC101 was demonstrated [40, 41]. Although at t28 no effect on inflammatory gene expression could be seen in the vein grafts, blockade of the binding of VEGF to VEGFR2 inhibited macrophage influx and subsequent effects on plaque composition including increased collagen and smooth muscle cell content. The NF-κB signaling cascade is an obvious route, since NF-κB induced inflammation has been previously reported to be a critical pathway to stimulate macrophage influx and plaque instability in vein grafts [24, 36, 42].

In this study we used a vein graft model in hypercholesterolemic mice to study the role of plaque neovessel maturation. This model shows large atherosclerotic lesions with abundant plaque

angiogenesis [23]. Vein graft atherosclerosis differs from native atherosclerosis since the onset (surgery) is acute with endothelial denudation and hypoxia resulting in the accelerated form. The lesions formed are concentric and highly dispersed with inflammatory cells and foam cells [36]. Local processes regarding plaque neovessel maturation in vein grafts show high similarities with native atherosclerosis as demonstrated in figure 1. The findings in this study can be, with cause, extrapolated to other cardiovascular diseases.

In summary, VEGFR2 blocking antibodies inhibit intraplaque hemorrhage and erythrocyte extravasation, resulting in more stable plaque neovascularization, decreased lesion development and increased plaque stabilization in a vein graft model, due to maturation of the plaque neovessels. Our study indicates that vascular maturation (and more specifically VEGFR2) stands as an attractive target to stabilize atherosclerotic (vein graft) disease.

References

[1] de Vries MR, Quax PH. Plaque angiogenesis and its relation to inflammation and atherosclerotic plaque destabilization. *Current opinion in lipidology* 2016; **27**:499-506.
[2] Derksen WJ, Peeters W, van Lammeren GW *et al.* Different stages of intraplaque hemorrhage are associated with different plaque phenotypes: a large histopathological study in 794 carotid and 276 femoral endarterectomy specimens. *Atherosclerosis* 2011; **218**:369-377.
[3] Taqueti VR, Di Carli MF, Jerosch-Herold M *et al.* Increased microvascularization and vessel permeability associate with active inflammation in human atheromata. *Circ. Cardiovasc. Imaging* 2014; **7**:920-929.
[4] Yahagi K, Kolodgie FD, Otsuka F *et al.* Pathophysiology of native coronary, vein graft, and in-stent atherosclerosis. *Nature reviews. Cardiology* 2016**13**:79-98.
[5] de Vries MR, Simons KH, Jukema JW *et al.* Vein graft failure: from pathophysiology to clinical outcomes. *Nature reviews. Cardiology* 2016; **13**:451-470.
[6] Parma L, Baganha F, Quax PHA, de Vries MR. Plaque angiogenesis and intraplaque hemorrhage in atherosclerosis. *European journal of pharmacology* 2017;**5**:107-115.
[7] Lee ES, Bauer GE, Caldwell MP, Santilli SM. Association of artery wall hypoxia and cellular proliferation at a vascular anastomosis. *The Journal of surgical research* 2000; *91*:32-37.
[8] Wan J, Lata C, Santilli A *et al.* Supplemental oxygen reverses hypoxia-induced smooth muscle cell proliferation by modulating HIF-alpha and VEGF levels in a rabbit arteriovenous fistula model. *Annals of vascular surgery* 2014; **28**:725-736.
[9] Sluimer JC, Gasc JM, van Wanroij JL *et al.* Hypoxia, hypoxia-inducible transcription factor, and macrophages in human atherosclerotic plaques are correlated with intraplaque angiogenesis. *J. Am. Coll. Cardiol* 2008; **51**:1258-1265.
[10] Vazao H, Rosa S, Barata T *et al.* High-throughput identification of small molecules that affect human embryonic vascular development. *Proceedings of the National Academy of Sciences of the United States of America* 2017; **114**:E3022-e3031.
[11] Sluimer JC, Kolodgie FD, Bijnens AP *et al.* Thin-walled microvessels in human coronary atherosclerotic plaques show incomplete endothelial junctions relevance of compromised structural integrity for intraplaque microvascular leakage. *J. Am. Coll. Cardiol* 2009; **53**:1517-1527.
[12] Virmani R, Kolodgie FD, Burke AP *et al.* Atherosclerotic plaque progression and vulnerability to rupture: angiogenesis as a source of intraplaque hemorrhage. *Arterioscler. Thromb. Vasc. Biol* 2005; **25**:2054-2061.
[13] Michel JB, Virmani R, Arbustini E, Pasterkamp G. Intraplaque haemorrhages as the trigger of plaque vulnerability. Eur. Heart J 2011;**32**:1977-1985.
[14] Finn AV, Nakano M, Narula J *et al.* Concept of vulnerable/unstable plaque. *Arterioscler. Thromb. Vasc. Biol* 2010; **30**:1282-1292.
[15] Guo L, Akahori H, Harari E *et al.* CD163+ macrophages promote angiogenesis and vascular permeability accompanied by inflammation in atherosclerosis. *The Journal of clinical investigatio*n 2018; **128**:1106-1124.
[16] Carmeliet P, Jain RK. Molecular mechanisms and clinical applications of angiogenesis. *Nature* 2011; **473**:298-307.
[17] Huang Y, Goel S, Duda DG *et al.* Vascular normalization as an emerging strategy to enhance cancer immunotherapy. *Cancer research* 2013; **73**:2943-2948.
[18] Jain RK. Molecular regulation of vessel maturation. *Nat. Med* 2003; **9**:685-693.
[19] Jain RK. Antiangiogenesis strategies revisited: from starving tumors to alleviating hypoxia. *Cancer Cell* 2014; **26**:605-622.
[20] Moulton KS, Heller E, Konerding MA *et al.* Angiogenesis inhibitors endostatin or TNP-470 reduce intimal neovascularization and plaque growth in apolipoprotein E-deficient mice. *Circulation* 1999; **99**:1726-1732.
[21] Lucerna M, Zernecke A, de NR *et al.* Vascular endothelial growth factor-A induces plaque expansion in ApoE knock-out mice by promoting de novo leukocyte recruitment. *Blood* 2007; **109**:122-129.
[22] Xu X, Mao W, Chai Y *et al.* Angiogenesis Inhibitor, Endostar, Prevents Vasa Vasorum Neovascularization in a Swine Atherosclerosis Model. *Journal of atherosclerosis and thrombosis* 2015; **22**:1100-1112.
[23] de Vries MR, Niessen HW, Lowik CW *et al.* Plaque rupture complications in murine atherosclerotic vein grafts can be prevented by TIMP-1 overexpression. *PLoS. One* 2012; **7**:e47134.

[24] Wezel A, de Vries MR, Maassen JM *et al.* Deficiency of the TLR4 analogue RP105 aggravates vein graft disease by inducing a pro-inflammatory response. *Scientific reports* 2016; **6**:24248.
[25] Witte L, Hicklin DJ, Zhu Z *et al.* Monoclonal antibodies targeting the VEGF receptor-2 (Flk1/KDR) as an anti-angiogenic therapeutic strategy. *Cancer Metastasis Rev* 1998; **17**:155-161.
[26] Eefting D, Bot I, de Vries MR *et al.* Local lentiviral short hairpin RNA silencing of CCR2 inhibits vein graft thickening in hypercholesterolemic apolipoprotein E3-Leiden mice. *J. Vasc. Surg* 2009; **50**:152-160.
[27] Hamdan AD, Aiello LP, Misare BD *et al.* Vascular endothelial growth factor expression in canine peripheral vein bypass grafts. *Journal of vascular surgery* 1997; **26**:79-86.
[28] Falcon BL, Chintharlapalli S, Uhlik MT, Pytowski B. Antagonist antibodies to vascular endothelial growth factor receptor 2 (VEGFR-2) as anti-angiogenic agents. *Pharmacology & therapeutics* 2016; **164**:204-225.
[29] Winkler F, Kozin SV, Tong RT *et al.* Kinetics of vascular normalization by VEGFR2 blockade governs brain tumor response to radiation: role of oxygenation, angiopoietin-1, and matrix metalloproteinases. *Cancer Cell* 2004; *6*:553-563.
[30] Post S, Peeters W, Busser E *et al.* Balance between angiopoietin-1 and angiopoietin-2 is in favor of angiopoietin-2 in atherosclerotic plaques with high microvessel density. J. Vasc. Res 2008; 45:244-250.
[31] Van der Veken B, De Meyer GRY, Martinet W. Axitinib attenuates intraplaque angiogenesis, haemorrhages and plaque destabilization in mice. *Vascular pharmacology* 2018; **100**:34-40.
[32] Huang Y, Yuan J, Righi E *et al.* Vascular normalizing doses of antiangiogenic treatment reprogram the immunosuppressive tumor microenvironment and enhance immunotherapy. *Proceedings of the National Academy of Sciences of the United States of America* 2012; **109**:17561-17566.
[33] Asahara T, Bauters C, Pastore C *et al.* Local delivery of vascular endothelial growth factor accelerates reendothelialization and attenuates intimal hyperplasia in balloon-injured rat carotid artery. *Circulation* 1995; **91**:2793-2801.
[34] Luo Z, Asahara T, Tsurumi Y *et al.* Reduction of vein graft intimal hyperplasia and preservation of endothelium-dependent relaxation by topical vascular endothelial growth factor. *J. Vasc. Surg* 1998; **27**:167-173.
[35] Lardenoye JH, de Vries MR, Lowik CW *et al.* Accelerated atherosclerosis and calcification in vein grafts: a study in APOE*3 Leiden transgenic mice. Circ. Res 2002; 91:577-584.
[36] de Vries MR, Quax PHA. Inflammation in Vein Graft Disease. *Frontiers in cardiovascular medicine* 2018; **5**:3.
[37] Bates DO. Vascular endothelial growth factors and vascular permeability. *Cardiovascular research* 2010; **87**:262-271.
[38] Kockx MM, Cromheeke KM, Knaapen MW *et al.* Phagocytosis and macrophage activation associated with hemorrhagic microvessels in human atherosclerosis. *Arterioscler. Thromb. Vasc. Biol* 2003; **23**:440-446.
[39] Kim I, Moon SO, Kim SH *et al.* Vascular endothelial growth factor expression of intercellular adhesion molecule 1 (ICAM-1), vascular cell adhesion molecule 1 (VCAM-1), and E-selectin through nuclear factor-kappa B activation in endothelial cells. *The Journal of biological chemistry* 2001; **276**:7614-7620.
[40] Watanabe H, Mamelak AJ, Wang B *et al.* Anti-vascular endothelial growth factor receptor-2 (Flk-1/KDR) antibody suppresses contact hypersensitivity. *Experimental dermatology* 2004; **13**:671-681.
[41] Barbay V, Houssari M, Mekki M *et al.* Role of M2-like macrophage recruitment during angiogenic growth factor therapy. *Angiogenesis* 2015; **18**:191-200.
[42] Karper JC, de Vries MR, van den Brand BT *et al.* Toll-like receptor 4 is involved in human and mouse vein graft remodeling, and local gene silencing reduces vein graft disease in hypercholesterolemic APOE*3Leiden mice. *Arterioscler. Thromb. Vasc. Biol* 2011; **31**:1033-1040.

Supplemental material

STable 1. **Patient characteristics saphenous vein grafts**

Age	Sex	% stenosis	%stenosis bypass	Stage	Smoker	Diabetes I	Diabetes II	HLP	Previous MI	Heart Failure	CAD	Renal failure	Hypertension
58	male	60	30	Intermediate	no	no	no	no	yes	no	yes	no	yes
54	male	80-90	80	Late	no	no	no	no	no	no	no	no	no
37	male	60	75	Late	no	no	no	no	no	no	no	no	no
58	male	60	75	Late	no	no	no	no	no	no	no	no	no
92	male	40	40	Intermediate	no	no	no	no	no	no	yes	no	no
76	male	70	70	Late	no	no	no	no	no	no	yes	no	no
62	male	50	70	Late	no	no	yes	yes	no	no	yes	no	yes
62	male	50	25	Early	yes	no	no	no	no	no	yes	no	yes
62	male	80	70	Late	yes	no	no	no	no	no	yes	no	yes
70	female	60	40	Intermediate	no	no	no	no	no	no	no	no	no
70	female	30	30	Early	no	no	no	no	no	no	no	no	no
76	male	70	35	Intermediate	no	no	no	no	no	no	no	no	no

Abbreviations: HLP – hyperlipoproteinemia; MI – myocardial infarction; CAD – coronary artery disease. I n red photographs in figure 1, panel 1.

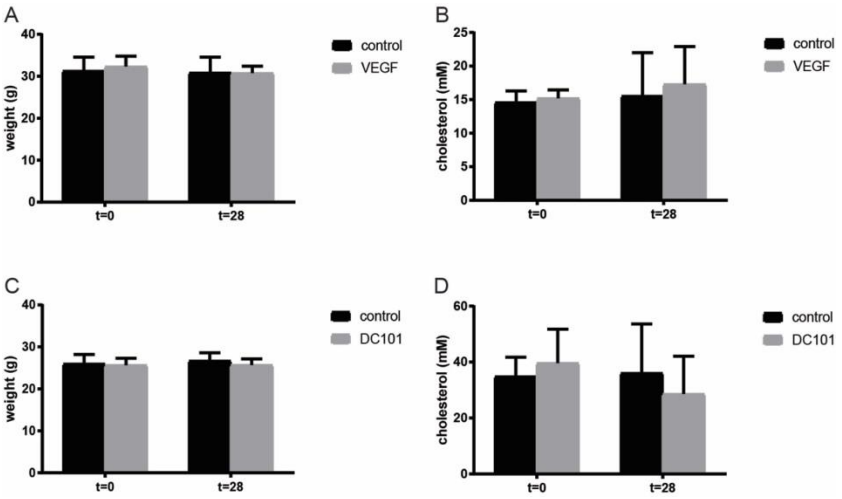

S1. **Bodyweight and cholesterol levels**. (**A**). Bodyweight before (t=0) and 28 days after surgery (t=28) of VEGF treated and control mice. (**B**). Plasma cholesterol levels before (t=0) and 28 days after surgery (t=28) of VEGF treated and control mice. (**C**). Bodyweight before (t=0) and 28 days after surgery (t=28) of VEGFR2 blocking antibodies (DC101) treated and control mice. (**D**). Plasma cholesterol levels before (t=0) and 28 days after surgery (t=28) of DC101 treated and control mice.

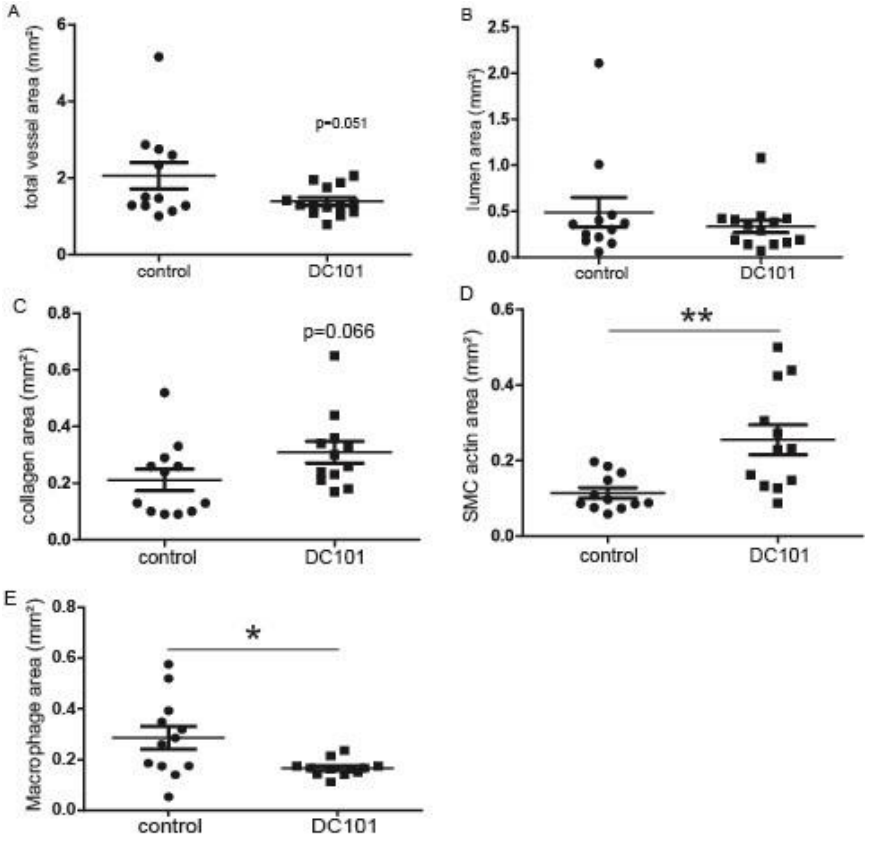

S2. **Vein graft morphometry**. Quantitative measurements of vein graft area and lesion composition in vein grafts in hypercholesterolemic ApoE3*L mice treated with control IgG antibodies (10 mg/kg) n=12 and VEGFR2 blocking antibodies (DC101, 10 mg/kg) n=14, 28 days after surgery. Quantitative measurements of (A) total vessel area, (B) luminal area, (C) collagen area, (D) smooth muscle cell (SMCA) area, (E)macrophage content. * $p<0.05$, ** $p<0.01$.